ELSEVIER

The role of ceria-based nanostructured materials in energy applications

M. Melchionna and P. Fornasiero*

Department of Chemical and Pharmaceutical Sciences, INSTM, ICCOM-CNR, University of Trieste, Via L. Giorgieri 1, 34127 Trieste, Italy

Ceria (CeO_2) is enjoying increasing popularity in catalytic applications, and in some cases has established itself as an irreplaceable component. The reasons for such success stem from the intrinsic structural and redox properties of ceria. Reducing the ceria particles to the nanoscale has a profound impact on the catalytic behavior. The proliferation of improved synthetic methods that allow control over the final morphology and size of the nano-structures is opening new possibilities in terms of catalytic potential, particularly for energy-related applications.

Introduction

The fast growth rate of the world population is one of the core factors accounting for the exponential increase in the yearly energy consumption. As of today, the main energy sources fulfilling global demands derive from stock or fossil fuels. However, there are rising concerns over the projected shortage of such energy supplies at the current level of *per capita* usage.

For this reason, the discovery of alternative energy sources has become a main priority in the scientific community, prompting the development of new technologies able to quench the energy thirst in the short- to medium-term future. In particular, emphasis is being given to those technological discoveries that embrace sustainability and environmental issues; in this context, there is large consensus among researchers that renewable energy sources are the only way forward to guarantee the consistent welfare of human society [1,2].

Since the 1980s, cerium dioxide, commonly known as ''ceria'', has established its role as one of the most promising materials for environmental and energy applications. From an environmental point of view, CeO_2 (and more specifically the mixed oxide CeO_2–ZrO_2) has gained an irreplaceable role as a promoter in three-way catalysts (TWCs) for the emission control of auto-exhaust polluting gases [3–5]. In addition to this major application, there are significant examples where CeO_2-based systems have proved to be outstanding components in the energy sector. In this context, the latest advances have converged towards one desirable characteristic: the reduction of CeO_2 structure size to the nanoscale level.

The goal of this review is to provide some key examples on the synthetic methods to access nano-structured ceria and their use as building blocks in the hierarchical assembly of high-ordered structures. Finally, energy applications where CeO_2 nanostructures are increasingly acquiring a central role will be highlighted.

Key properties of CeO_2

Cerium has two stable oxidation states, +4 and +3, and the relatively ease of switching between these two states is the essential factor for its catalytic activity. This rapid change of oxidation state is related to its ability to store and release oxygen, a property measured by the ''oxygen storage capacity'' (OSC). The typical fluorite-type structure of CeO_2 is retained through the temperature range from room temperature to the melting point. However, the Ce–O phase diagrams show that under reduction conditions, CeO_2 can release oxygen, undergoing phase transformations to a series of reduced oxides (CeO_{2-x}). The process is reversible and the re-oxidation to CeO_2 occurs at higher oxygen pressures [6]. In other words, ceria can act as an efficient oxygen buffer (Fig. 1).

The mobility of oxygen ions in ceria materials is another essential aspect for catalysis and electrochemical purposes [7]. Oxygen ion diffusion is closely linked to the structural defects present in the materials [8]. Distinctive types of defects that are important in catalytic applications are the oxygen vacancies ($V_o^{\bullet\bullet}$), which can be introduced by doping the ceria lattice with oxides of metals with oxidation state lower than (IV) and lead to enhanced ionic

*Corresponding author. Fornasiero, P. (pfornasiero@units.it)

1369-7021/ http://dx.doi.org/10.1016/j.mattod.2014.05.005

Please cite this article in press as: M. Melchionna, P. Fornasiero, Mater. Today (2014), http://dx.doi.org/10.1016/j.mattod.2014.05.005

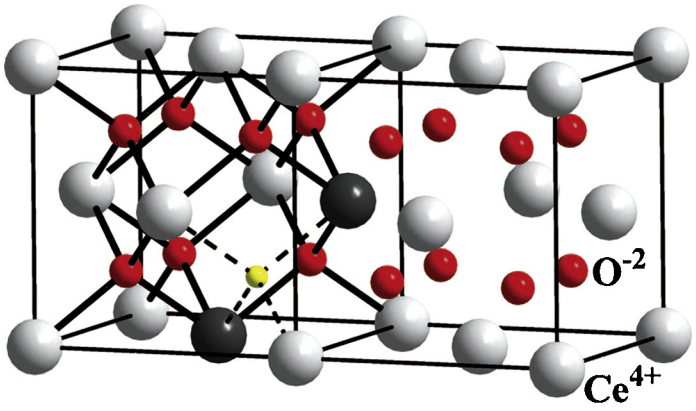

FIGURE 1

Crystal structure of doped ceria, showing undoped CeO_2 (right cube), and lanthanide-doped CeO_2 (left cube) with an oxygen vacancy (small sphere). Reprinted from ref. [10] with permission from the Copyright (2006) National Academy of Sciences, USA.

conductivity [9,10]. It is worth mentioning that other molecules can be stored within the ceria bulk, and be exploited for important energy- or environmental-related catalysis. For example, CO is one molecule that can be readily stored and this gives rise to the possibility of using ceria-based materials for processes such as CO preferential oxidation (CO-PROX) [11,12]. The stored CO can also be used to reduce environmentally malign species such as NO [13]. Quantum mechanical simulations have been used to explain the mechanism of the storage, release and transport [14].

Nano-structured ceria-based materials: synthetic methods

Upon decrease of the particle size, distinct physical and chemical properties as compared to bulk materials arise. One such property, very important in catalysis, is an increase of lattice constants (lattice relaxation), associated with the compositional and local structural changes from fluorite-type (CeO_2) to sesquioxide-type (Ce_2O_3), and consequently an increase of the oxygen vacancy content [15,16]. Hence, mobility of oxygen ions is increased.

Tailoring the shape of the nanoparticles has become a central consideration in the assembly of CeO_2-based materials. Indeed, despite the cubic phase of the fluorite structure and therefore its isotropicity, the different facets are not equal with respect to the atomic arrangement. As a result, maximization of the exposure of certain facets can lead to significant improvements in catalytic performances. Efforts are being made to find a correlation between the surface science relative to the exposed facets and the material science for heterogeneous catalysis [17]. The surface chemistry of ceria also includes theoretical studies [18].

The development of a large arsenal of synthetic methods for the preparation of CeO_2 nanoparticles has given access to a variety of geometries including materials with zero-, one-, two- and three-dimensional control of nanostructures [19].

Zero-dimensional (0D) nanoparticles are most straight forward to obtain, given the absence of a preferential growth direction of the fluorite-type seeding crystals. Trivially, CeO_2 nanopolyhedra are synthesized by applying standard protocols applied to nanoparticles of other materials. Co-precipitation exploits the extremely low solubility of ceria and is a simple and valuable technique. It is carried out in alkaline solutions with NaOH [20], urea [21], ammonia [22], etc. as precipitating agents. To avoid quick precipitation of too small-sized crystals the presence of surfactants such as cetyltrimethylamonium bromide (CTAB) [23] or polyvinylpyrrolidone (PVP) [24] is required, allowing better control of the particles dimensions.

Structures of higher dimensional complexity (1D, 2D and 3D) are synthetically more demanding and require accurate fine-tuning of reaction conditions. Their preparation is based on the two-stage sequence of nucleation and controlled crystal growth, both important to determine the final architecture. During nucleation, formation of many small crystallites takes place, and surface energies play a pivotal role in ensuring crystal size increase. In the second stage, aggregation of the crystals occurs and needs to be controlled in order to direct the assembly towards the desired structure.

1D CeO_2 nano-particles undoubtedly represent the most studied type of structure on account of their peculiar physical properties and their potential as components in nanodevices [25]. Accessible architectures include nanowires, nanotubes, nanorods and nanospindles and many 1D materials have been reported, together with studies of the mechanisms of formation [26,27].

In general terms, the assembly relies on two approaches differing in whether the procedure involves use of a surfactant or not.

Surfactant-free methods exploit capping agents that can specifically protect some facets during nucleation, thus altering surface energies and breaking the isotropicity of the face-center cubic system. Even simple counter-anions such as Cl^- and NO_3^- have been shown to direct the synthesis towards nanospheres, nanowires or nanorods by preferential interaction of the anion with one crystallographic facet (Fig. 2) [28,29].

In the surfactant-assisted approach, instead, the role of the surfactant is to act as a template, favoring anisotropic growth along a specific direction by spatial confinement (hard template method) or by means of preferential interaction of one surface plane with surfactant micelle systems that spontaneously self-assemble into 1D structures at critical concentrations (soft template method).

Popular hard templates for 1D geometries include anodic aluminium oxide (AAO) [30] and polycarbonate membrane filters [31]. Carbon nanotubes (CNTs) have also emerged as intriguing removable templates [32,33].

Templating by soft surfactants appears to be a more versatile method to build mono-dimensional arrangements, and a large variety of soft templates has been reported to efficiently assist formation of 1D morphologies. Common soft templates include CTAB, oleylamine, polyvinylpyrrolidone (PVP), ethylenediamine, ethylene glycol, alkyltrimethylammonium salts and others.

It must be noted that the (soft) template approach is a general technique and features chemical species that are not specific for a single type of structure, but the final geometry rather evolves by the applied synthetic conditions. Therefore, several parameters such as temperature, reaction time, cerium precursor, surfactant/cerium ratio, pH, etc. can decisively affect the final outcome, with discrimination also encompassing possible 2D and 3D structures formation.

Indicative examples include the formation of CeO_2 nanowires and nanorings assisted by sodium bis(2-ethylhexyl)sulfosuccinate (NaAOT) [34,35] and the ethylene glycol-mediated assembly of

Please cite this article in press as: M. Melchionna, P. Fornasiero, Mater. Today (2014), http://dx.doi.org/10.1016/j.mattod.2014.05.005

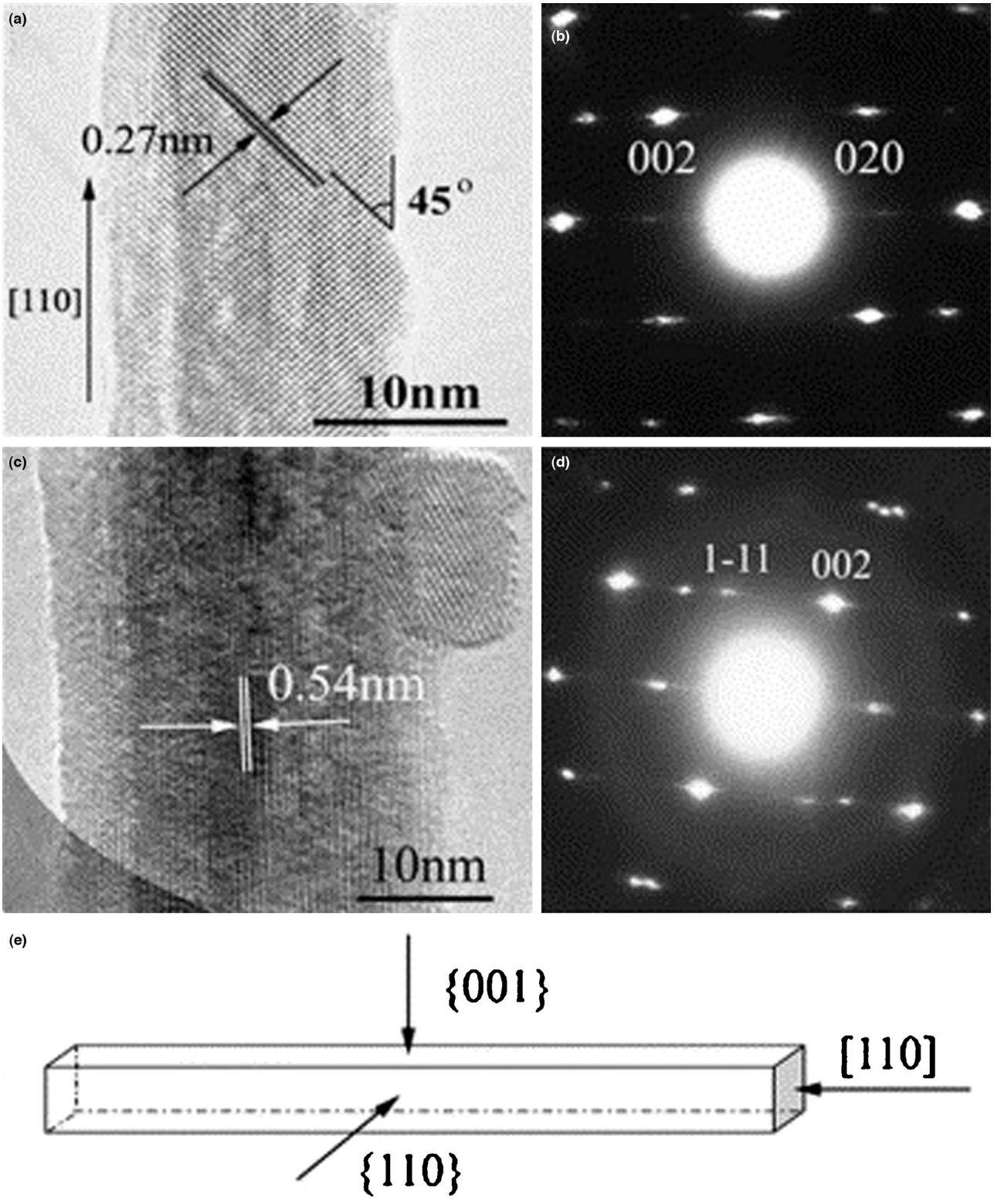

FIGURE 2

HRTEM of a typical nanorod view along {0 0 1} direction (a) and corresponding SAED pattern (b); HRTEM image of a typical nanorod view along {1 1 0}(c) and corresponding SAED pattern (d); (e) structural model of CeO_2 nanorods. Reprinted from Ref. [29] with permission from Elsevier Ltd.

Please cite this article in press as: M. Melchionna, P. Fornasiero, Mater. Today (2014), http://dx.doi.org/10.1016/j.mattod.2014.05.005

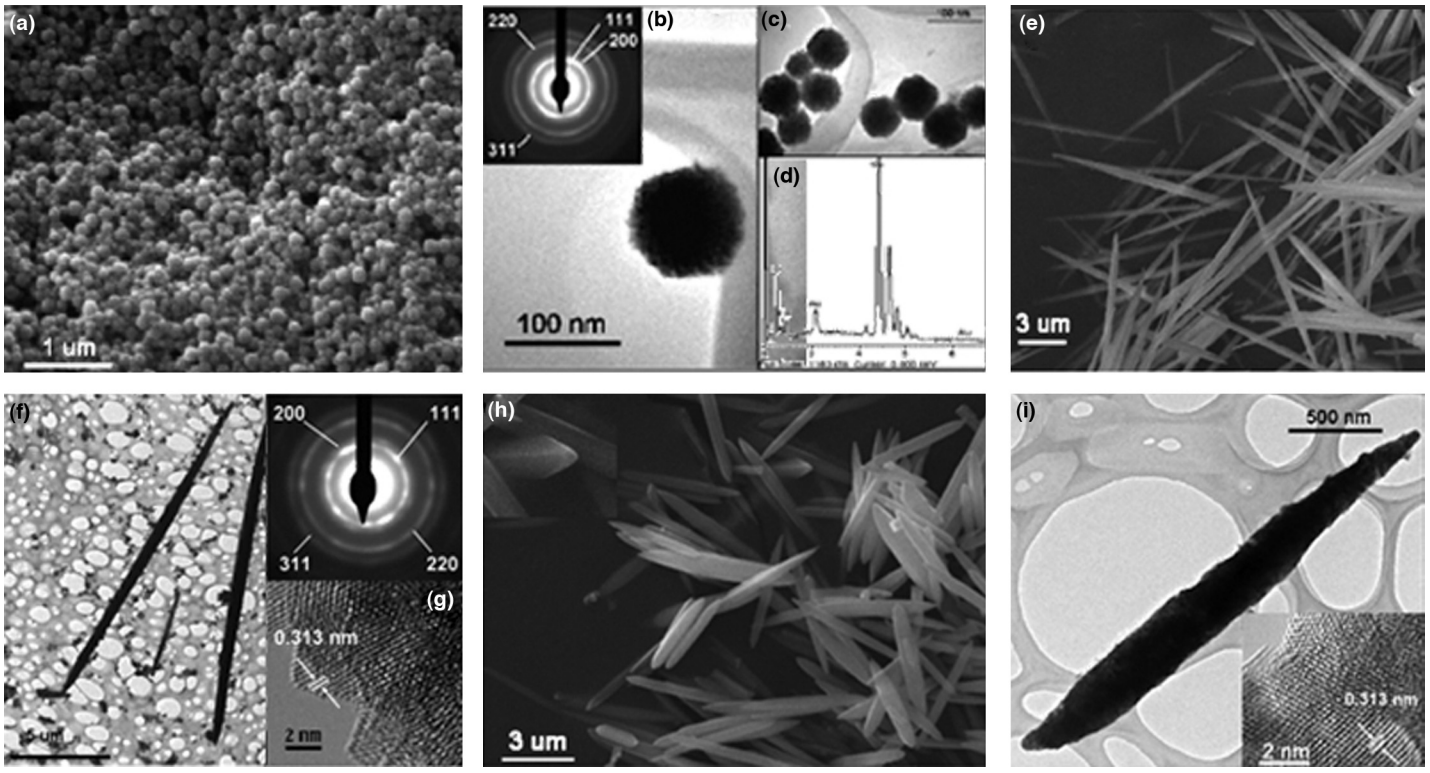

FIGURE 3

(a) SEM of annealed CeO_2 nanospheres; (b and c) CeO_2 nanospheres TEM images and its electron diffraction pattern (d); EDX of nanospheres, (e) SEM and (f) TEM images of annealed CeO_2 microrods, (g) HRTEM image of CeO_2 microrods, (h) SEM image of CeO_2 spindle-like particles and (i) TEM and HRTEM images (inset) of individual particles Reprinted with permission from Ref. [36]. Copyright 2005 American Chemical Society.

nanorods, nanospindles and nanospheres, where the final geometry is controlled by the reaction time and the concentration of the cerium precursor (Fig. 3) [36].

As far as 2D morphologies are concerned, the choice for the preparative protocol seems to be restricted to the template-assisted method, in view of the difficult control of the crystal growth rate along two or more facets. One template-free method to prepare disk-like morphologies was reported by Zhong *et al.* via solvothermal synthesis, with disks reaching micro-sized dimensions [37], while cobalt-doped CeO_2 nanostructures with disks and triangular shapes were attained by tuning the doping amount of cobalt nitrate through hydrothermal reaction [38]. 3D materials have been synthesized in several morphologies. One of the most investigated is the flower-like shape, which is gaining attention because it has been shown to possess significant physical properties related to its porosity and surface area. A multi-process complex mechanism has been proposed for the generation of three-dimensional hollow spheres with nano-petals possessing high surface area ($92.2\ m^2\ g^{-1}$), large pore volume ($0.17\ cm^3\ g^{-1}$), and marked hydrothermal stability (Fig. 4) [39].

Hard templates have also been used to prepare other 3D structures. By using silica spheres as templates, successively removed by

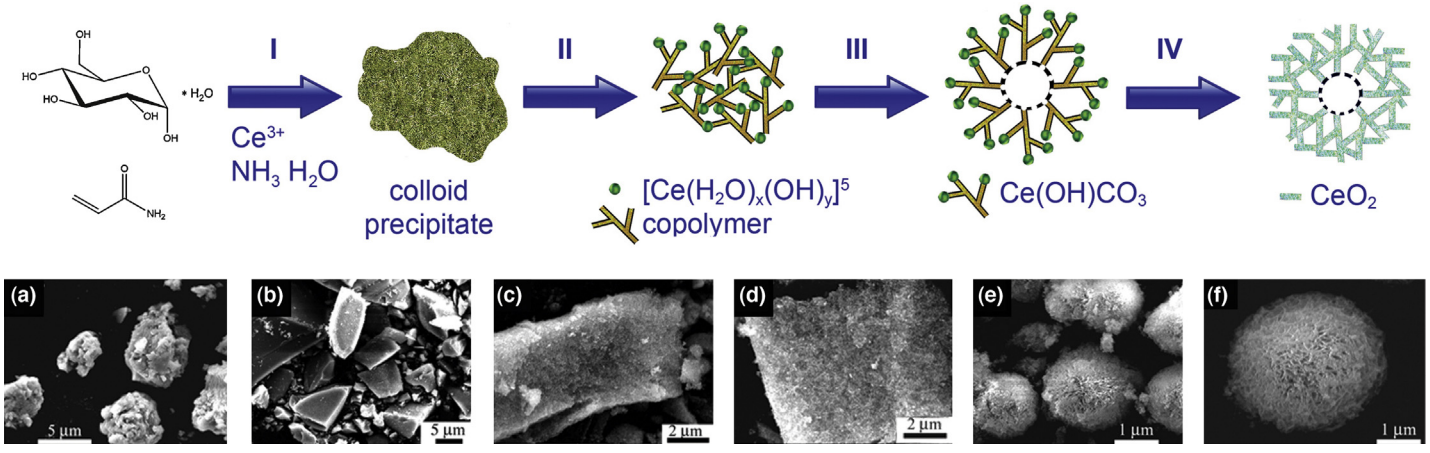

FIGURE 4

Top: Scheme of the evolution of flowerlike CeO2 microspeheres. Bottom: Morphology evolution. SEM images of the product obtained after (a) 0 h, (b) 3 h, (c) 6 h, (d) 9 h, (e) 12 h and (f) 18 h. Adapted with permission from ref. 39. Copyright 2006 American Chemical Society.

Please cite this article in press as: M. Melchionna, P. Fornasiero, Mater. Today (2014), http://dx.doi.org/10.1016/j.mattod.2014.05.005

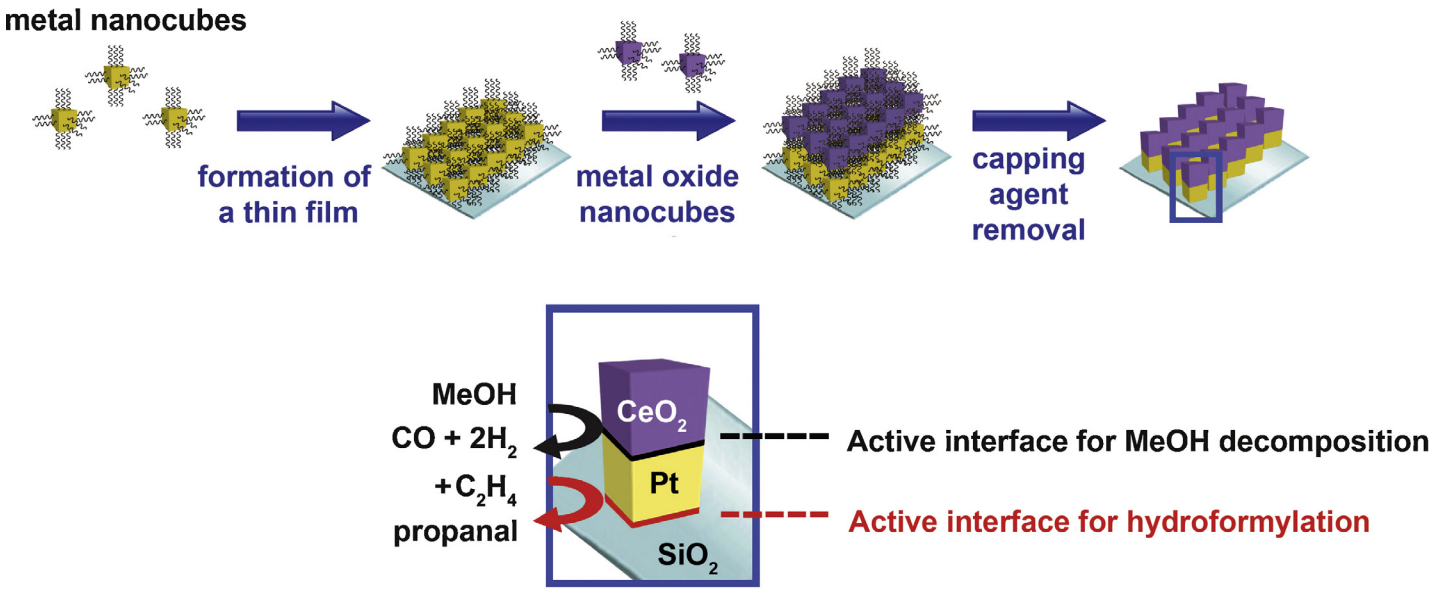

FIGURE 5

Assembly process for the preparation of a nanocrystal bilayer 'tandem catalyst'.

etching with NaOH solution, hollow nanospheres were successfully prepared [40].

Other 3D available structures include prisms and cubes. For example, cubes and three-dimensional octahedra were prepared by hydrothermal methods using different precursors [41], while prism-like structures have been reported to be selectively formed upon appropriate concentrations of OH^- [42].

Metal/ceria catalysts and hierarchical systems

In the vast majority of catalyst systems, CeO_2 is combined with another metal species that acts as the ''nominal'' active species, while ceria functions as support. The word ''nominal'' must be introduced because CeO_2 has a much more complex role. There is a demonstrated synergism between the support (that in these cases is referred to as ''active'') and the metal catalyst; [43] therefore the actual active species is the result of the interplay between the two phases, whose characteristics are merged rather than simply added up [44].

A representative example is the investigation of a Pt/CeO_2 system, where two types of oxidative metal–oxide interaction were identified, and the nanoscale effect for the oxygen transfer from the ceria to the Pt was proved, thus unravelling the mechanism of formation for the catalytically indispensable Pt–O species on ceria [45].

Another implicit aspect is that the as-prepared individual shapes almost invariably undergo an assembly process into larger architectures. For example, in the earlier description of 3D nano-flowers, it was implied that the final structure was actually the result of the supramolecular assembly of smaller building blocks. In some cases, the assembly can be controlled to a good extent; then the term ''hierarchal'' system is commonly used, to emphasize a process where the building blocks assemble in an ordered fashion leading to specific types of larger architectures.

The hierarchical assembly of ceria-based materials offers an immense potential in application-driven fields as the selectivity and performance of the component can be tailored by accurately devising the order of assembly of individual subunits. Yamada *et al.* harnessed a hierarchical assembly where Pt nanocubes were bi-dimensionally layered onto a flat SiO_2 sheet, followed by deposition of CeO_2 nanocubes. In this way, the Pt catalyst has a double Pt–metal oxide interface and can act as a tandem catalyst for the sequential two-step sequence of CH_3OH decomposition to CO and H_2 ($Pt–CeO_2$), and the hydroformilation of ethylene ($Pt–SiO_2$) (Fig. 5) [46].

One special type of hierarchical system involves formation of core-shell structures, where the metal nanoparticles are embedded into a ceria cocoon. A very versatile synthesis for materials with Pd and Pt has been developed, where core–shell subunits can be further stabilized by immobilization over Al_2O_3 [47]. By utilizing a silane-modified Al_2O_3, the same types of core–shells were singly deposited and exhibited exceptional stability and activity in the oxidation of methane, which was completed at temperatures below 400 °C. The noble metal nanoparticles escaped agglomeration even at calcination temperatures as high as 850 °C due to the effective protection of the CeO_2 shell and the efficient immobilization on the modified alumina (Fig. 6) [48].

Energy applications

With regards to energy applications, H_2 production/purification undoubtedly represents an exciting opportunity where nanostructured CeO_2 materials play a significant role. Fuel cells [49,50] and photocatalytic water splitting are equally attracting a great deal of attention [51,52].

H_2 production

The incorporation of ceria-based materials, particularly ceria–zirconia mixed oxides, into the formulation of reforming catalysts has been proved to endow the catalytic systems with additional advantages in terms of activity and stability [53].

Ethanol is the most investigated fuel on account of its environmentally low impact. As several products (such as acetone and acetaldehyde) are formed during ethanol reforming, another key

Please cite this article in press as: M. Melchionna, P. Fornasiero, Mater. Today (2014), http://dx.doi.org/10.1016/j.mattod.2014.05.005

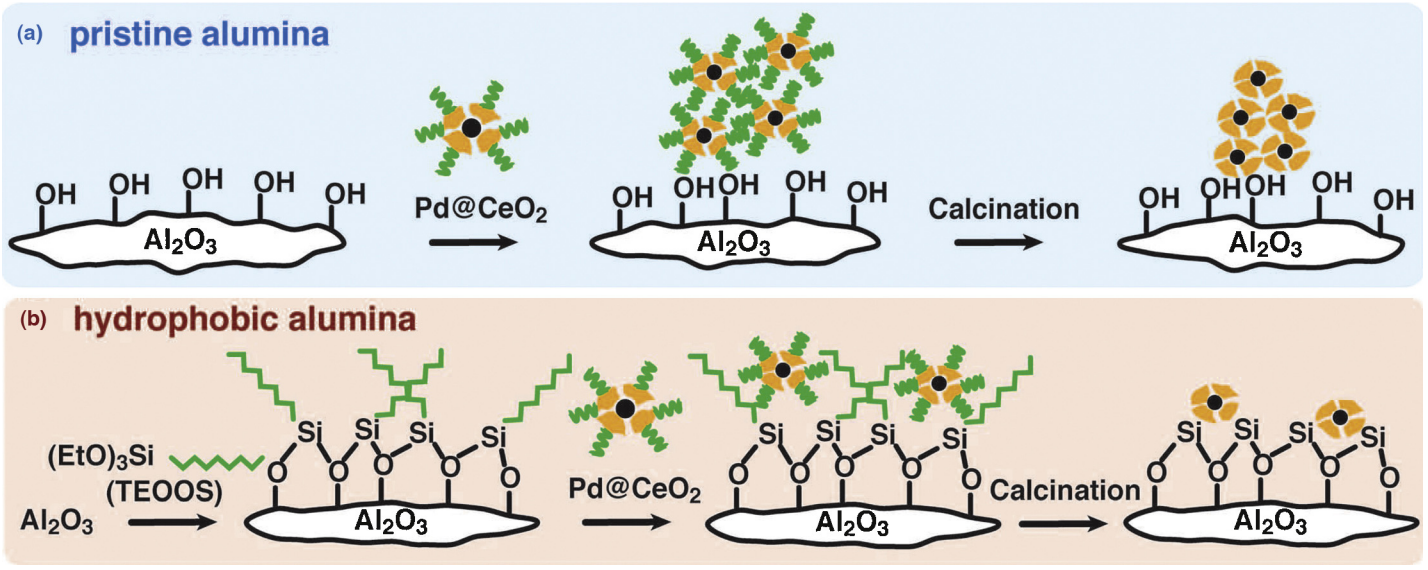

FIGURE 6

Schematic representation of the agglomeration of $Pd@CeO_2$ structures with the pristine alumina (a) and their deposition as single units after treatment of the same support with triethoxy(octyl)silane (TEOOS) (b). From ref [48]. Reprinted with permission from AAAS.

issue is the selectivity of the catalyst. Outstanding H_2 formation was reported by using a catalyst featuring CeO_2–Cu. Together with a concentration of hydrogen as high as 74%mol at relatively low temperatures, neither traces of the ketone or aldehyde by-product nor CO were detected. The great stability and selectivity of the product was put in relation to the flower-shaped nano-structure of the catalytic system [39].

Rh/CeO_2 nanocube and nanorod catalysts were also proved to be superior catalysts for steam reforming as compared to irregularly arranged ceria nanoparticles. Moreover, the different behaviors of cubes vs rods strongly suggest a dependence upon the crystallographic facets ({1 1 0} and {1 0 0} for nanorods and {1 0 0} for nanocubes as measured by HRTEM analysis) exposed by the two structures (Fig. 7) [54].

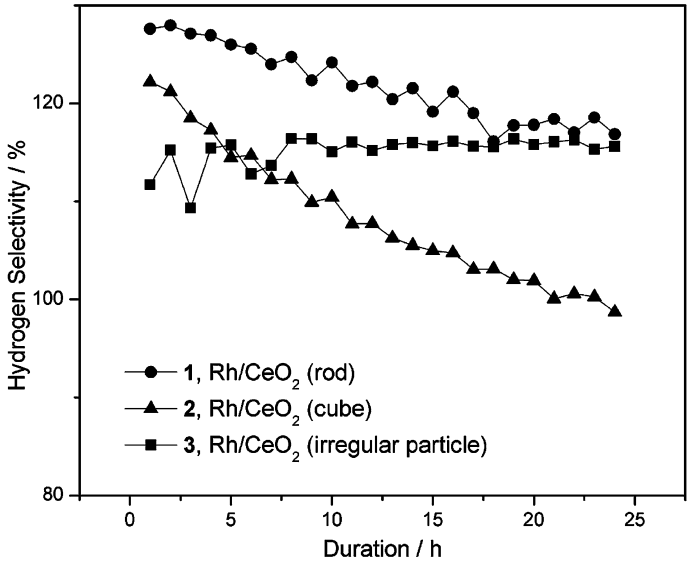

FIGURE 7

H_2 selectivities of the different Rh/CeO_2 structures as a function of duration on stream Reprinted from ref. [54] with permission from Elsevier Ltd.

Although less attractive due to higher toxicity issues, reforming methanol is another option that generally brings higher H_2 evolution rates. For instance, Au-loaded ceria nanocubes and nanorods were investigated, with the latter displaying good activities and selectivities, while the former turned out to be totally inactive [55].

H_2 purification

Water gas shift (WGS, Eq. (1)) and preferential oxidation (PROX, Eq. (2)) are two important reactions, used to reduce the levels of CO formed during H_2 production.

$$CO + H_2 \leftrightarrow CO_2 + H_2 WGS \quad (1)$$

$$CO + 1/2O_2 \rightarrow CO_2 PROX(\text{inlarge} H_2 \text{excess}) \quad (2)$$

Purification of H_2 by means of (a combination of) these two processes is crucial as the presence of CO can poison the metal catalyst, affecting considerably the efficiency.

WGS is carried out in two stages: high-temperature (between 300 and 450 °C) and low temperature (between 200 and 300 °C). Ceria appears to be particularly useful in the low-temperature process, and it is normally used as a support for loading noble metal catalysts (typically Pt, Au, Cu).

Nanostructured ceria-based composites using Au as the catalyst have drawn attention as the most promising systems for CO oxidation [56]. A classic example refers to the study carried out by Fu *et al.* where gold–ceria materials displayed high activities for WGS below 300 °C and the activity was dependent upon the size of the ceria particles [57]. Other reports confirmed the importance of nano-crystalline CeO_2 for the enhancement in catalytic performance [58]. Systems featuring nanocrystalline Pt and Au supported on nano-structured ceria were investigated and was suggested that the metallic nanoparticles are mere spectators in the WGS reaction, while the active species seems to be evolving by association of non-metallic ionic Pt and Au species with cerium–oxygen groups [59]. On the other hand, time-resolved X-ray

Please cite this article in press as: M. Melchionna, P. Fornasiero, Mater. Today (2014), http://dx.doi.org/10.1016/j.mattod.2014.05.005

diffraction and X-ray absorption spectroscopy studies indicate that pure gold nanoparticles in contact with oxygen vacancies can be involved as active species [60]. However, research in this area is very active and it has been demonstrated that various factors can correlate with the activity in the WGS reaction and the mechanism is still under debate.

Similar to the WGS, Au–CeO_2 materials have proved to be superior systems for PROX reactions. DFT calculations were used to explain the higher Au activity *vs* Pt-based systems [61], while comparison studies of Au/ceria and CuO/ceria in PROX reactions showed a higher activity for the Au-based system while selectivity was in favor of the CuO/ceria catalyst [62]. Once again, such study relates to specific synthetic protocols of the two catalysts and much care should be taken before drawing general trends. The effect of doping the ceria support with Sm^{3+}, La^{3+} and Zn^{2+} was also investigated while employing nanostructured Au/CeO_2 catalysts for PROX, resulting in either higher (Sm^{3+} and Zn^{2+}) or lower (La^{3+}) performances under the conditions used [63]. Enhanced stabilization of the Au catalyst towards sintering was achieved by embedding the Au NPs in highly porous nanocrystalline ceria, resulting in materials with good activities and excellent thermal stability [64].

Fuel cells

Ceria has been successfully integrated in several types of fuel cells. Solid oxide fuel cells (SOFCs), are very attractive on account of their benign environmental impact. In fact, the overall products of SOFCs are simply electricity, water and heat.

These types of cell offer one more specific advantage, namely the possibility of using a variety of fuels, including CO, given that their functioning does not rely on the use of a noble metal, in contrast with other types of fuel cells. On the other hand, they are characterized by an elevated operative temperature that can reach values as high as 1000 °C; this introduces a limitation as start-up and shut-down times are too long; moreover, the component materials are subjected to thermal stress. Therefore, one research challenge currently lies in the development of low temperature solid oxide fuel cells (LTSOFCs). In this context, ceria nanomaterials are being extensively explored as electrolytes with improved ionic conductivity. The enhancement in conductivity arises from larger contribution of the grain-boundary conductivity in comparison with traditional polycrystalline solids. In this region, nano-electrolytes exhibit faster oxygen ion diffusion than in the bulk, in contrast with conventional micro-sized electrolytes [65,66].

When used as electrolyte, ceria is generally doped with another trivalent element (or less commonly bivalent), which results in significant improvement of the ionic conductivity. Doping augments the oxygen vacancy concentration, which dictate the ionic conduction, at least for cells composed of single phase electrolytes [67,68]. Typical dopants are Gd_2O_3 (GDC), Sm_2O_3 (SDC), Y_2O_3 (YDC) and CaO (CDC).

Further developments have led to the general consensus that two-phase electrolyte nanocomposites, where doped ceria is combined with carbonates (Fig. 8) [69,70], hydroxides [71], sulfates [72], halides [73] or oxides [74,75] results in an ionic conductivity that can overcome single phase doped ceria by up to 10 orders of magnitude. Other than as electrolyte, ceria is being widely investigated as electrode component [76]. It has been demonstrated that integration of ceria allows the use of carbon-based fuels because of its resistance to carbon deposition. For example, a Pd–CeO_2 core–shell system layered on a yttria-stabilized zirconia (YSZ) anode was proved to increase considerably the performance in SOFC. The system is effective either with H_2 or CH_4 as fuels, displaying a higher dispersion of the Pd@CeO_2 NPs in comparison with bare Pd NPs. Dispersion was maintained at high temperature under both oxidative (calcination) and operative reduction conditions (Fig. 9) [77].

The geometry of the nano-structured CeO_2 also appears to be a parameter that can lead to improved performances. Li *et al.* prepared flower-like structures of CeO_2 and combined it with Ru to assemble an iso-octane reforming catalyst that was applied to a conventional anode of a SOFC. This was a structural variation to the original work by Bernett *et al.* [50], and led to a significant performance enhancement.

The utilization of CeO_2 as components in anodic electrocatalysts has also been accomplished for polymer electrolyte-membrane fuel cells (PEMFCs). By supporting Pd nanoparticles

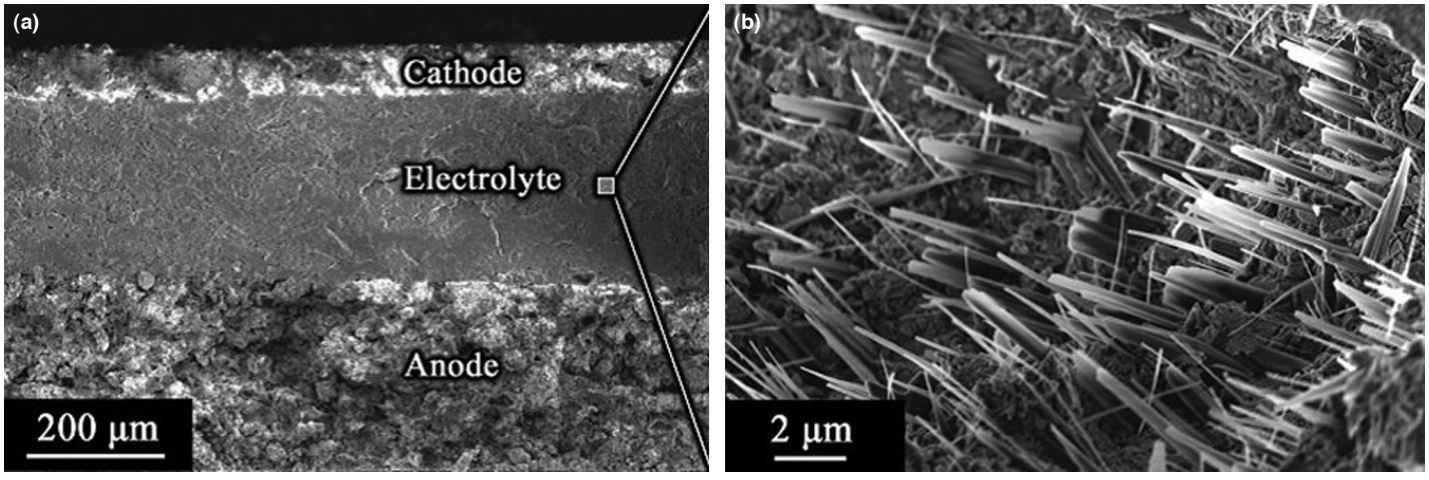

FIGURE 8

SEM images of single SOFC with doped ceria nanowire-carbonate electrolyte Reprinted from Ref. [70] with permission. Copyright 2010 Wiley.

Please cite this article in press as: M. Melchionna, P. Fornasiero, Mater. Today (2014), http://dx.doi.org/10.1016/j.mattod.2014.05.005

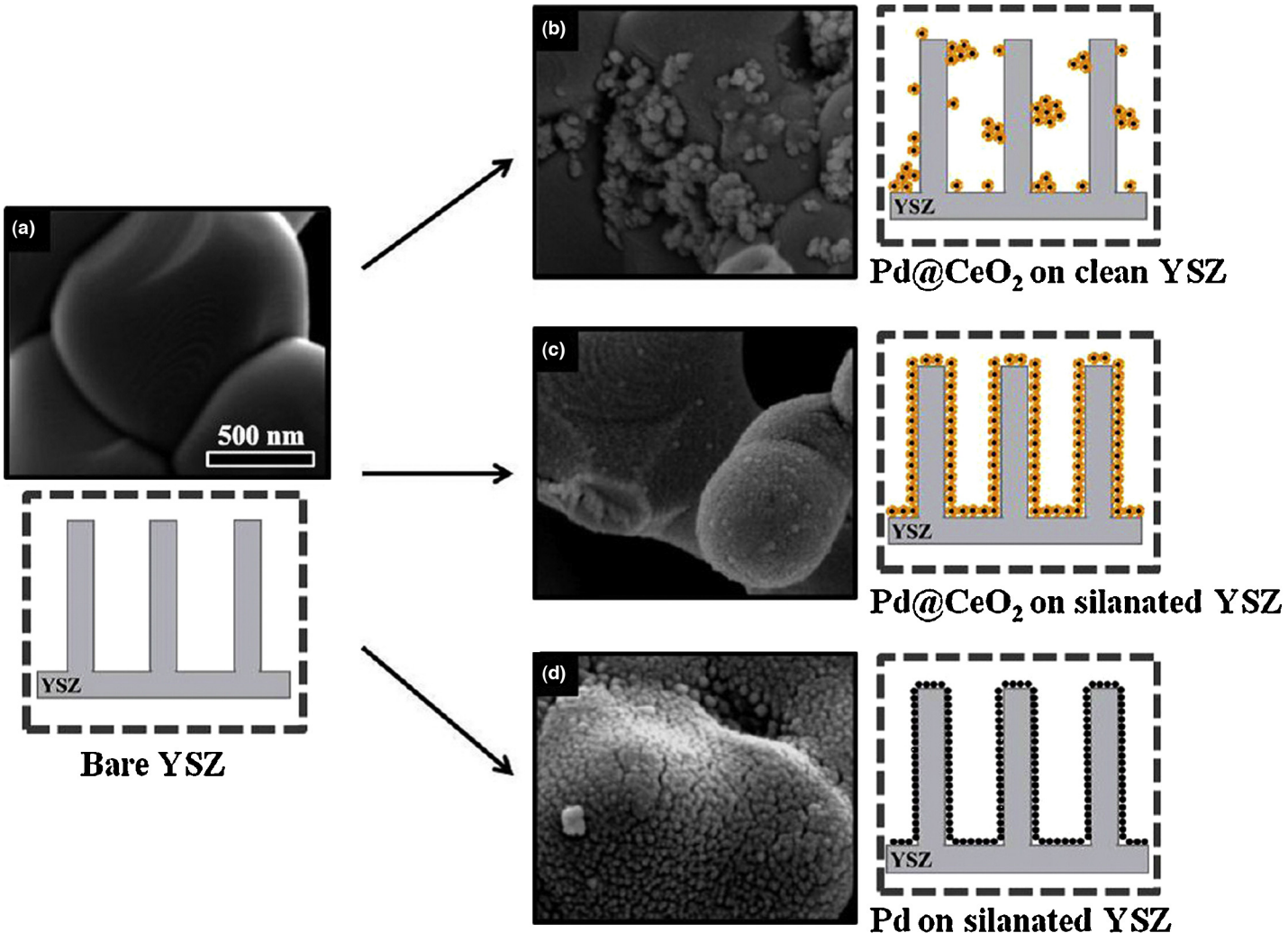

FIGURE 9

Structural comparison (schematic representations and corresponding TEM images) of the different YSZ anodes, emphasizing the best dispersion obtained using Pd@CeO_2 on silanated YSZ. Reprinted with permission from Ref. [77]. Copyright 2013 American Chemical Society.

on a mixed CeO_2/carbon black, the direct oxidation of ethanol fuel was carried out with double performance in comparison with standard Pd/carbon black catalysts [78].

Photocatalytic water splitting

Exciting opportunities arise from the activity of ceria in photo-induced processes. Corma *et al*. had demonstrated a photovoltaic response for nanometre sized CeO_2 particles, which could ultimately be exploited to construct an organic dye-free solar cell [79]. In the context of photocatalysis, however, ceria seems to be particularly intriguing in the water splitting process, for the generation of H_2. The effect of doping in ceria–zirconia mixed oxides was explored in two-step photocatalytic water splitting, while nanoparticulate CeO_2 was used as a support to deposit Au NPs, and the system exhibited higher efficiency than the standard WO_3 when irradiated with visible light ($\lambda > 400$ nm) (Fig. 10) [80].

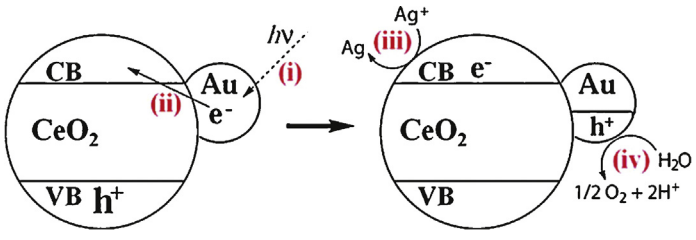

FIGURE 10

Scheme of the water splitting process by Au supported on ceria showing the: (i) Photon absorption; (ii) electron injection from Au to ceria conduction band; (iii) electron quenching by Ag^+; (iv) water oxidation by h^+. Reprinted with permission from Ref. [80]. Copyright 2011 American Chemical Society.

An electrochemical synthesis of CeO_2 nanorods on Ti substrates was shown to result in predominant exposure of the {1 1 0} planes which turned out to be the photocatalytically active facet for the H_2 evolution, and the authors related the activity to the special redox properties of the CeO_2 component [81].

Conclusions and perspectives

Nano-structured CeO_2 has thoroughly proved its central role as a versatile and superior active catalytic support for energy processes. Enormous advances have been made in the control over the shape, size and composition of CeO_2-based materials. However, there is still margin for synthetic optimization, particularly with an eye to

Please cite this article in press as: M. Melchionna, P. Fornasiero, Mater. Today (2014), http://dx.doi.org/10.1016/j.mattod.2014.05.005

the economy of the preparative protocols for large scale production and real implementation at an industrial level. In this context, the stability of the as-prepared materials in a large spectrum of operative conditions will also be of paramount importance.

More reliable tuning of the properties of the final composites, such as the defect levels and oxygen ions/vacancies densities, as well as the inherent reactivity of crystal facets and their exposure to the reaction media are additional parameters that could be better controlled.

Focus should also be placed on gaining a comprehensive knowledge of the structure/performance relationship. In this respect, in-depth mechanistic details of the crosstalk at the interface between the ceria and the other active components would constitute invaluable assets toward the design of catalysts with enhanced activities and selectivities. Given the rapid progress in the establishment of improved characterization techniques and theoretical analyses, such information appears to be well within reach: it is therefore likely that we will soon be witnessing new important breakthroughs in this fascinating research area.

Acknowledgements

We kindly acknowledge FP7-NMP-2012-SMALL-6 (project ID 310651) and HI-PHUTURE (protocol 2010N3T9M4) for financial support.

References

[1] Renewable Resources and Renewable Energy: A Global Challenge, Taylor & Francis, Boca Raton, FL, 2011.
[2] J. Kaspar, P. Fornasiero, M. Graziani, Catal. Today 2 (1999) 285–298.
[3] A. Trovarelli, Catal. Rev. Sci. Eng. 38 (1996) 439–520.
[4] P. Fornasiero, et al. J. Catal. 187 (1999) 177–185.
[5] G. Vlaic, et al. J. Catal. 182 (1999) 378–389.
[6] M. Zinkevich, D. Djurovic, F. Aldinger, Solid State Ionic 177 (2006) 989–1001.
[7] L. Malavasi, et al. Chem. Soc. Rev. 39 (2010) 4370–4387.
[8] M.V. Ganduglia-Pirovano, et al. Surf. Sci. Rep. 62 (2007) 219–270.
[9] M. Mogensen, N.M. Sammes, G.A. Tompsett, Solid State Ionic 129 (2000) 63–94.
[10] K. Schwarz, Proc. Natl. Acad. Sci. U.S.A. 103 (2006) 3497.
[11] C. Mondelli, et al. Catal. Today 113 (2006) 81–86.
[12] M. Boaro, et al. Appl. Catal. B: Environ. 52 (2004) 225–237.
[13] X. Yao, et al. Catal. Sci. Technol. 3 (2013) 1355–1366.
[14] N.V. Skorodumova, et al. Phys. Rev. Lett. 89 (2002) 166601.
[15] S. Tsunekawa, et al. Appl. Surf. Sci. 152 (1999) 53–56.
[16] X.D. Zhou, W. Huebner, Appl. Phys. Lett. 79 (2001) 3512–3514.
[17] K. Zhou, Y. Li, Angew. Chem. Int. Ed. 51 (2012) 602–613.
[18] J. Paier, et al. Chem. Rev. 113 (2013) 3949–3985.
[19] C. Sun, et al. Energy Environ. Sci. 5 (2012) 8475–8505.
[20] M. Yamashita, et al. J. Mater. Sci. 37 (2002) 683–687.
[21] M.S. Tsai, Mat. Sci. Eng. B-Solid 110 (2004) 132–134.
[22] X.D. Zhou, W. Huebner, H.U. Anderson, Appl. Phys. Lett. 80 (2002) 3814–3816.
[23] G.F. Wang, et al. J. Alloys Compd. 493 (2010) 202–207.
[24] Y.S. Chaudhary, et al. J. Mater. Chem. 20 (2010) 2381–2385.
[25] L. Liao, et al. J. Phys. Chem. C 112 (2008) 9061–9065.
[26] S. Chowdhury, K.-S. Lin, J. Nanomater. (2011), Article ID 157690.
[27] K.S. Lin, S. Chowdhury, Int. J. Mol. Sci. 11 (2010) 3226–3251.
[28] W. Wang, et al. J. Mater. Chem. 20 (2010) 7776–7781.
[29] K.B. Zhou, et al. J. Catal. 229 (2005) 206–212.
[30] T. Yang, D.G. Xia, Mater. Chem. Phys. 123 (2010) 816–820.
[31] M. Boehme, et al. Nanotechnology 22 (2011) 065602.
[32] D.S. Zhang, et al. Micropor. Mesopor. Mat. 117 (2009) 193–200.
[33] D.S. Zhang, et al. Carbon 44 (2006) 2853–2855.
[34] M. Yada, et al. Adv. Mater. 16 (2004) 1222–1226.
[35] C. Sun, et al. Chem. Lett. 33 (2004) 662–663.
[36] C. Ho, et al. Chem. Mater. 17 (2005) 4514–4522.
[37] J.J. Chen, et al. Powder Technol. 197 (2010) 136–139.
[38] X.-H. Guo, et al. Small 10 (2012) 1515–1520.
[39] C.W. Sun, et al. J. Phys. Chem. B 110 (2006) 13445–13452.
[40] N.C. Strandwitz, G.D. Stucky, Chem. Mater. 21 (2009) 4577–4582.
[41] Z.L. Wu, et al. Langmuir 26 (2010) 16595–16606.
[42] X.W. Lu, et al. J. Alloys Compd. 476 (2009) 958–962.
[43] S. Bernal, et al. Catal. Today 50 (1999) 175–206.
[44] M. Cargnello, et al. Science 341 (2013) 771–773.
[45] G.N. Vayssilov, et al. Nat. Mater. 10 (2011) 310–315.
[46] Y. Yamada, et al. Nat. Chem. 3 (2011) 372–376.
[47] M. Cargnello, et al. J. Am. Chem. Soc. 132 (2010) 1402–1409.
[48] M. Cargnello, et al. Science 337 (2012) 713–717.
[49] S.D. Park, J.M. Vohs, R.J. Gorte, Nature 404 (2000) 265–267.
[50] Z. Zhan, S.A. Barnett, Science 308 (2005) 844–847.
[51] A. Kudo, Y. Miseki, Chem. Soc. Rev. 38 (2009) 253–278.
[52] P.V. Kamat, J. Phys. Chem. C 111 (2007) 2834–2860.
[53] T. Montini, et al. Appl. Catal. B: Environ. 71 (2007) 125–134.
[54] W.I. Hsiao, et al. Chem. Phys. Lett. 441 (2007) 294–299.
[55] N. Yi, R. Si, H. Saltsburg, M. Flytzani-Stephanopoulos, Energy Environ. Sci. 3 (2010) 831–837.
[56] M. Haruta, et al. Chem. Lett. 16 (1987) 405–408.
[57] Q. Fu, A. Weber, M. Flytzani-Stephanopoulos, Catal. Lett. 77 (2001) 87–95.
[58] S. Carrettin, et al. Angew. Chem. Int. Ed. 43 (2004) 2538–2540.
[59] Q. Fu, H. Saltsburg, M. Flytzani-Stephanopoulos, Science 301 (2003) 935–938.
[60] J.A. Rodriguez, et al. Top. Catal. 44 (2007) 73–81.
[61] S. Kandoi, et al. Catal. Lett. 93 (2004) 93–100.
[62] G. Avgouropoulos, et al. Chem. Eng. J. 124 (2006) 41–45.
[63] M. Manzoli, et al. Catal. Today 138 (2008) 239–243.
[64] M. Cargnello, et al. Chem. Mater. 22 (2010) 4335–4345.
[65] X. Guo, et al. Solid State Ionics 555 (2002) 154–155.
[66] H.L. Tuller, Solid State Ionics 131 (2000) 143–157.
[67] G. Mogensen, M. Mogensen, Thermochim. Acta 214 (1993) 47–50.
[68] S. Deshpande, et al. Appl. Phys. Lett. 87 (2005) 133113.
[69] B. Zhu, J. Power Sources 114 (2003) 1–9.
[70] Y. Ma, et al. Adv. Funct. Mat. 22 (2010) 1640–1644.
[71] J. Hu, et al. J. Power Sources 154 (2006) 106–114.
[72] X.R. Liu, et al. Eng. Mater. 280–283 (2004) 425–430.
[73] B. Zhu, et al. J. Mater. Sci. Lett. 20 (2001) 591–594.
[74] J. Huang, et al. Int. J. Hydrogen Energy 37 (2012) 13044–13052.
[75] R. Raza, et al. Solid State Ionics 188 (2011) 58–63.
[76] M. Mogensen, J. Electrochem. Soc. 141 (1994) 2122–2128.
[77] L. Adijanto, et al. ACS Catal. 3 (2013) 1801–1809.
[78] V. Bambagioni, et al. ChemSusChem 5 (2012) 1266–1273.
[79] A. Corma, et al. Nat. Mater. 3 (2004) 394–397.
[80] A. Primo, et al. J. Am. Chem. Soc. 133 (2011) 6930–6933.
[81] X. Lu, et al. J. Mater. Chem. 21 (2011) 5569–5572.

Please cite this article in press as: M. Melchionna, P. Fornasiero, Mater. Today (2014), http://dx.doi.org/10.1016/j.mattod.2014.05.005